Available online at www.sciencedirect.com
ScienceDirect
Chinese Journal of Natural Medicines 2022, **20**(7): 551-560
doi: 10.1016/S1875-5364(22)60185-7
Chinese Journal of Natural Medicines

•Research article•

Deep chemical identification of phytoecdysteroids in *Achyranthes bidentata* Blume by UHPLC coupled with linear ion trap-Orbitrap mass spectrometry and targeted isolation

WANG Ying-Ying[1, 2Δ], LI Jia-Yuan[2Δ], YAO Chang-Liang[2], ZHANG Jian-Qing[2], YU Yang[2, 3], YAO Shuai[2], GAO Min[2, 3], WU Shi-Fei[2], WEI Wen-Long[2], BI Qi-Rui[2], GUO De-An[1, 2*]

[1] *School of Chinese Materia Medica, Nanjing University of Chinese Medicine, Nanjing 210023, China;*
[2] *Shanghai Research Center for Modernization of Traditional Chinese Medicine, Shanghai Institute of Materia Medica, Chinese Academy of Sciences, Shanghai 201203, China;*
[3] *School of Pharmaceutical Sciences, University of Chinese Academy of Sciences, Beijing 100049, China*

Available online 20 Jul., 2022

[ABSTRACT] *Achyranthes bidentata* Blume is widely used as a traditional Chinese medicine with the effects of nourishing the liver and kidneys and strengthening muscles and bones. In this work, a rapid and simple strategy was developed for characterizing phytoecdysteroids by ultra-high-performance liquid chromatography coupled with liner ion trap-Orbitrap mass spectrometry using electrospray ionization in the negative mode. As a result, 47 phytoecdysteroids were unambiguously or tentatively characterized. Among them, seven known compounds were identified according to the reference standards along with molecular formula, retention time and fragmentation patterns, while others were mostly potential new compounds. Through targeted isolation, the structures of three new compounds were determined by NMR spectra, which were consistent with LC-MS characterization. The present study provides an efficient method to deeply characterize phytoecdysteroids.

[KEY WORDS] *Achyranthes bidentata* Blume; Chemical identification; Fragmentation behaviors; Phytoecdysteroids; Targeted isolation

[CLC Number] R917, R284 **[Document code]** A **[Article ID]** 2095-6975(2022)07-0551-10

Introduction

Traditional medicines make use of natural products and is of great importance for the treatment of various diseases. Plenty of researches are engaged in exploring their secondary metabolites by various methods, such as chemical isolation along with nuclear magnetic resonance (NMR) based structural elucidation and mass spectrometry based identification [1-3]. Metabolite identification can be broadly categorized into four levels, namely identified compounds (level 1), putatively annotated compounds (level 2), putatively characterized compounds (level 3) and unknown compounds (level 4) [4]. Generally, NMR based structural elucidation corresponds to identified compounds (level 1), the highest level of identification. MS based identification usually leads to the second-class data (levels 2−4) without reference standards. Compared with tedious chemical isolation by which limited compounds are often obtained, MS identification after chromatographic separation (such as LC-MS) can provide a comprehensive profiling of the chemical components. Therefore, these two methods are often used in combination for different purposes.

Achyranthes bidentata Blume belongs to the family of Amaranthaceae, which is also known as "Huai Niu Xi" in Chinese. According to Chinese Pharmacopoeia (ChP, 2020 edition), Achyranthes Radix can be used to treat extravasated blood and hepatic and renal injury. It is widely distributed in most parts of China, and planted as a genuine regional herb in Henan Province. The extract of *A. bidentata* possesses a variety of pharmacological activities, such as inhibiting osteoporosis [5-7], anti-inflammation [8, 9] and analgesic [10] activity,

[Received on] 12-Jan.-2022
[Research funding] This work was supported by the National Key R&D Program of China (No. 2019YFC1711000), and the Qi-Huang Chief Scientist Program of National Administration of Traditional Chinese Medicine (2020).
[*Corresponding author] Tel/Fax: 86-21-5027-1516, E-mail: daguo@simm.ac.cn
[Δ]These authors contributed equally to this work.
These authors have no conflict of interest to declare.

improving learning and memory [11], antiviral activity [12], anti-tumor [13] and anti-oxidative [14, 15] effects.

As the main active constituents, twenty-five phytoecdysteroids were isolated and characterized from *A. bidentata* in total [16-19]. *β*-Ecdysterone, as a quality control marker of Achyranthes Radix, is designated to be not less than 0.030% in ChP 2020. The main structural characteristics of phytoecdysteroids include the *cis*-configuration of ring A/B, the *trans*-configuration of ring C/D, double bond mostly located on C-7, 8, carbonyl situated in C-6, and an eight-carbon polyol side chain of C-17. Despite explicit significance and characteristics of phytoecdysteroids, few methods were established to identify and characterize these substances. In the current study, a straightforward and validated strategy was established by characterizing the compounds with UHPLC-linear ion trap (LTQ)-Orbitrap and subsequent targeted isolation of the new compounds. The strategy was utilized to decipher phytoecdysteroids in *A. bidentata* for the first time.

Materials and Methods

Chemicals and reagents

The roots of *Achyranthes bidentata* Blume (batch number: 180401) were purchased from Guangdong Tiancheng Traditional Chinese Medicine Co., Ltd. (Guangdong, China), and identified by Prof. GUO De-An (Shanghai Institute of Materia Medica, Shanghai, China). A voucher specimen (HNX-180401) was deposited in Shanghai Research Center for Modernization of Traditional Chinese Medicine, Shanghai Institute of Materia Medica, Shanghai, China. Achyranthesterone A, podecdysone C, *β*-ecdysterone, polypodine B, makisterone A, 25*R*-inokosterone, and 25*S*-inokosterone were isolated and unambiguously identified by the authors.

HPLC-grade acetonitrile was obtained from Merck KGaA (Merck, Darmstadt, Germany), and LC-MS grade formic acid was supplied by Tokyo Chemical Industry Co., Ltd. (TCI, Tokyo, Japan). Ultrapure water was purified using a Milli-Q water purification system (Millipore, Billerica, MA, USA). Other solvents used in this experiment were of analytical grade and purchased from Sinopharm Shanghai Chemical Reagent Co., Ltd. (Shanghai, China).

Sample preparation

The powered roots of *A. bidentata* Blume (1.2 g) were first extracted with 70% EtOH (3 × 10 mL) by ultrasonics at room temperature for 10 min. Next, the combined extracts were evaporated to dryness in a water bath. Then the residue was dissolved with water and applied to a D101 macroporous column (2 cm × 10 cm) eluted with 200 mL of water, 20% EtOH and 80% EtOH in sequence. Then, the 20% EtOH elution was evaporated to dryness, redissolved in 1 mL of 70% EtOH and then centrifuged in 14 000 r·min^{-1} for 10 min. The resultant supernatant was stored at 4 °C prior to analysis.

UHPLC-LTQ/Orbitrap-MS analysis

Chromatographic separation was performed on Ultimate® 3000 UHPLC system (Thermo Fisher Scientific, San Jose, CA, USA) using a Waters ACQUITY UPLC HSS T3 column (2.1 mm × 100 mm, 1.8 μm; Waters, Milford, MA, USA) at 30 °C. Acetonitrile (solvent B) and 0.1% formic acid aqueous solution (solvent A) were used as mobile phases. The flow rate was set at 0.3 mL·min^{-1}, where the linear gradient was as follows: 0−3 min, 11%−13% B; 3−10 min, 13% B; 10−15 min, 13%−16% B; 15−20 min, 16%−35% B; 20−22 min, 35% B; 22−28 min, 35%−95% B; and 28−32 min, 95%−11% B. The injection volume was 1 μL.

The high-energy *C*-trap dissociation (HCD) fragmentation patterns of phytoecdysteroids were investigated on an LTQ-Orbitrap Velos Pro hybrid mass spectrometer (Thermo Fisher Scientific, San Jose, CA, USA) in the negative mode. The source parameters were set as follows: source spray voltage, 3.8 kV; capillary temperature, 320 °C; source heater temperature, 200 °C; auxiliary gas (N_2), 8 arbitrary units; and sheath gas (N_2), 15 arbitrary units. A duty cycle included four events (I−IV). Full scan over *m/z* 300−700 at a resolution of 30 000 (FWHM defined at *m/z* 400) was performed in Event I. Events II−IV recorded MS^2 spectrum of the most intense precursor ions from full scan at normalized collision energy (NCE) of 80/100/120 in HCD respectively. The profile format for MS scan and the centroid format for MS^2 were both recorded and processed with Xcalibur 2.1 software (Thermo Fisher Scientific, San Jose, CA, USA).

Results and Discussion

Identification of chemical constituents

After considering the MS/MS fragmentation behaviors and their substitution groups at C-21 and C-25, seven phytoecdysteroids standards were categorized into three classes (Supporting information Fig. S1). Class A: achyranthesterone A, which contained an OH group in the position of C-21. Class B: podecdysone C, *β*-ecdysterone, polypodine B and makisterone A, which contained OH in the position of C-25, without OH at C-21. Class C: 25*R*-inokosterone and 25*S*-inokosterone, which contained OH at neither C-21 nor C-25. The fragmentation behaviors of each type exhibited significant differences. Class A: it showed obvious neutral loss (NL) of 30 Da (CH_2O) [eg. *m/z* 175.10→145.09] in side chain due to the OH at C-21 (Fig. 1). Class B: characteristic NLs of 76 Da ($C_3H_8O_2$) [eg. *m/z* 159.10→83.05] and 92 Da ($C_3H_8O_3$) [eg. *m/z* 175.10→83.05] and diagnostic product ions (DPIs) of *m/z* 83.05 and 97.07 from side chains were observed. They were attributed to the presence of OH at C-25, and the easily broken bond between C-24 and C-25 (e.g. podecdysone C, Fig. 2). Class C: compared with classes A and B, compounds in class C did not display the above DPIs and NLs. As shown in Fig. 3, 25*S*-inokosterone generated the complementary ion pair at *m/z* 159.01 and 319.19 in MS/MS spectrum. Also, the common ions at *m/z* 141.09 and 301.18 were observed by the elimination of H_2O from *m/z* 159.01 and 319.19, respectively. Accordingly, 47 phytoecdysteroids were tentatively identified, including 5, 24 and 18 compounds in classes A, B and C, respectively (shown in

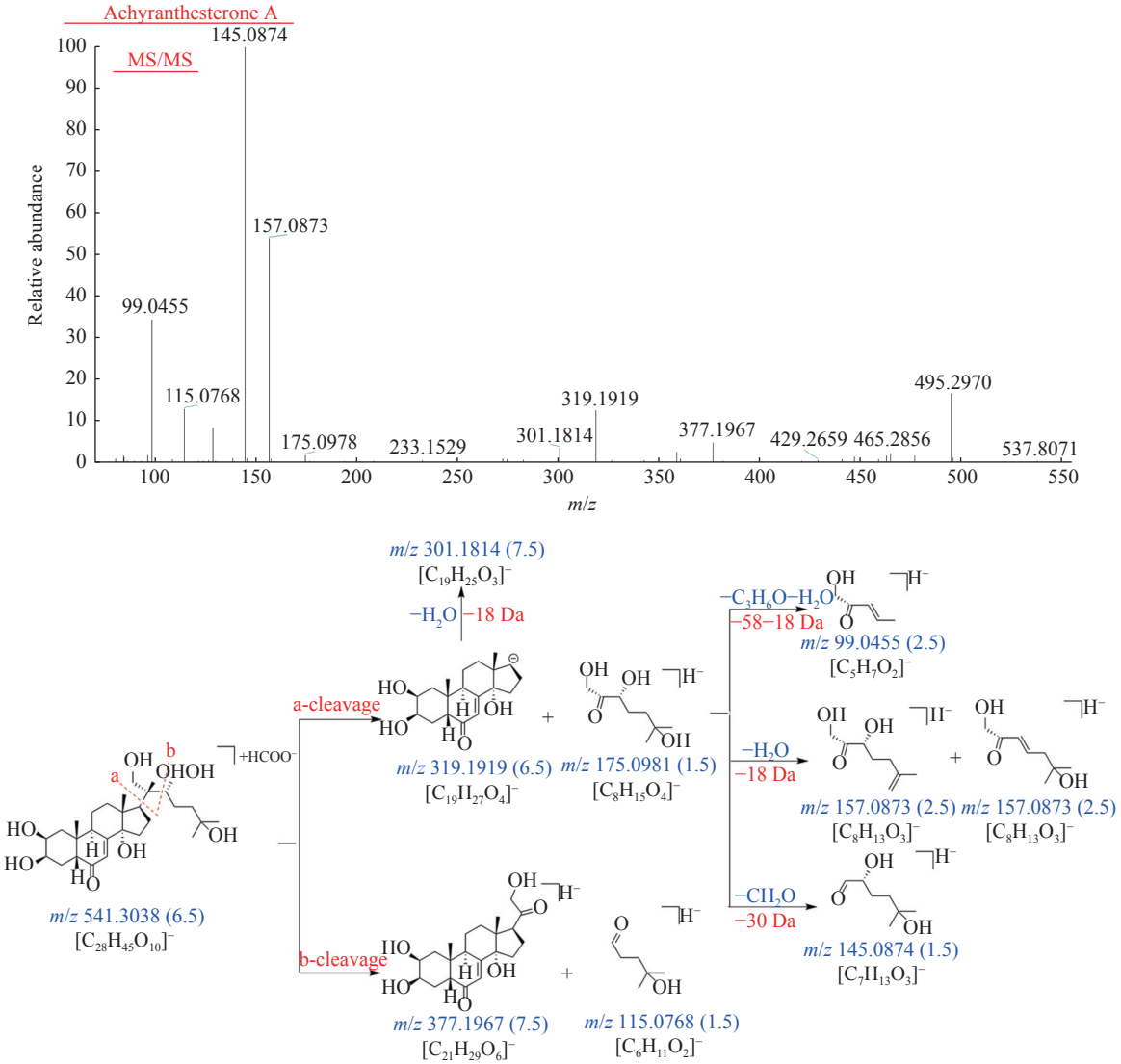

Fig. 1 The proposed MS fragmentation pathways of achyranthesterone A (the number in the parentheses shows RDBeq value)

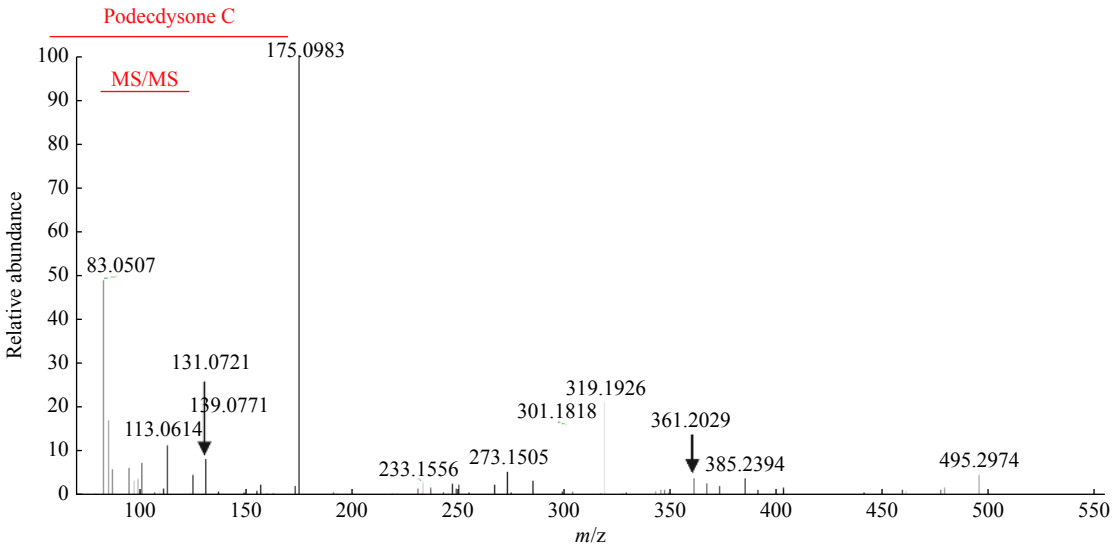

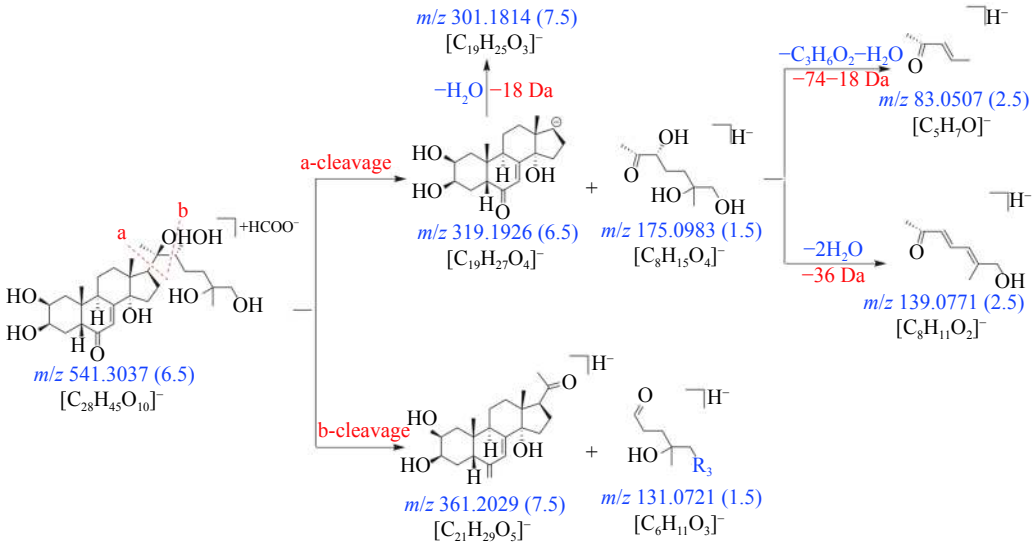

Fig. 2 The proposed MS fragmentation pathways of podecdysone C (the number in the parentheses shows RDBeq value)

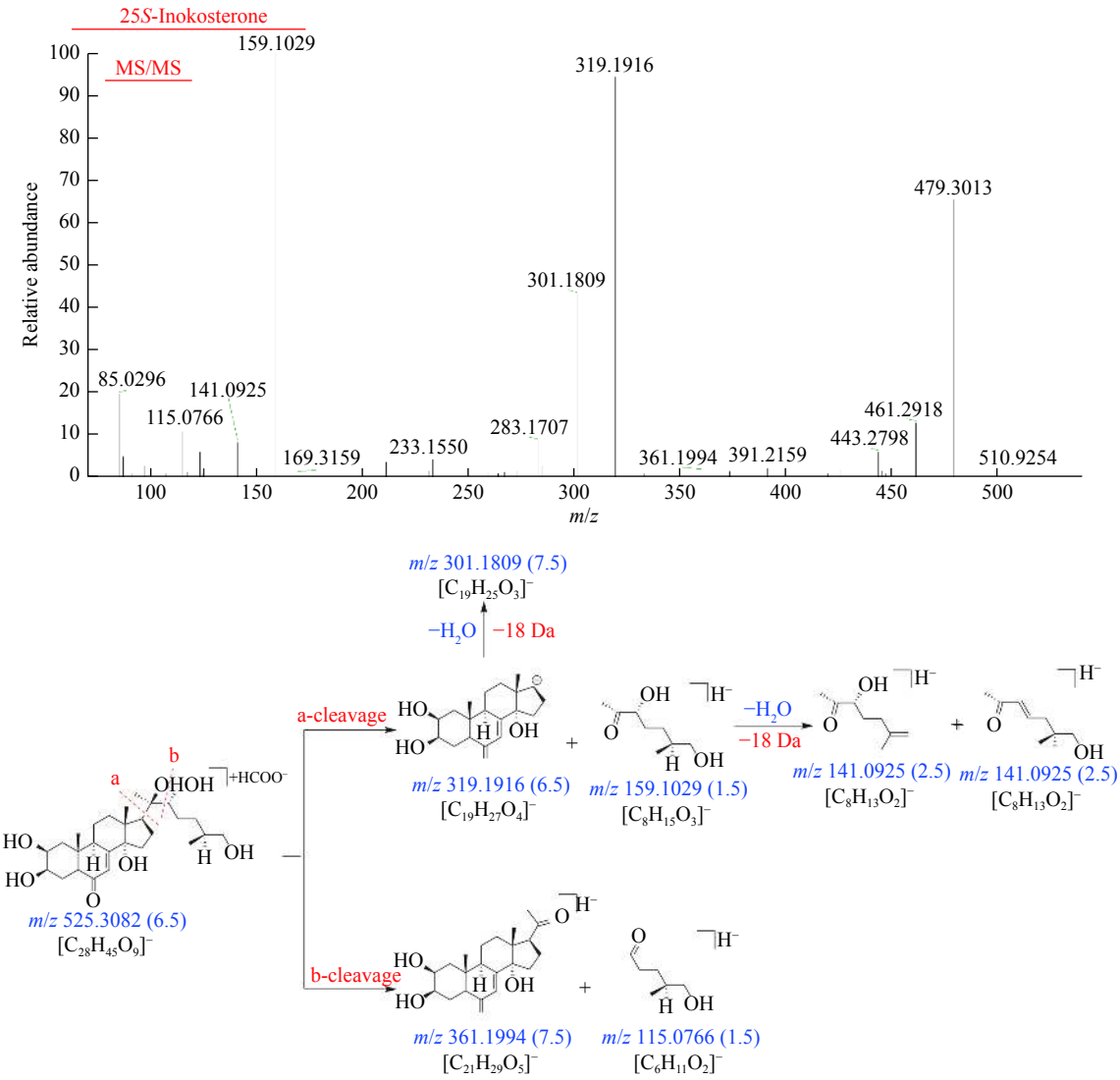

Fig. 3 The proposed MS fragmentation pathways of 25*S*-inokosterone (the number in the parentheses shows RDBeq value)

Table 1).

Characterization of compounds in class A

Compounds **A1**−**A5** were characterized as class A. Taking **A1** as an example, Fig. 4A illustrated the MS spectrum of **A1**. The molecular formula of **A1** was deduced as $C_{27}H_{44}O_8$ from $[M + HCOO]^-$ at *m/z* 541.3035. Its typical product ions at *m/z* 319.19, 175.10, 157.09, 145.10 and 99.05 were consistent with the skeleton and side chain of phytoecdysteroids.

Table 1 Structural identification of phytoecdysteroids and its glycosides in *A. bidentata*

No.	t_R/min	*m/z*	M − H	Adducts	Delta mmu	Molecular formula	MS/MS fragment ions	Identification	C21-OH	C25-OH
A1	9.2	541.304	495.2982	$+HCOO^-$	3.276	$C_{27}H_{44}O_8$	HCD80: 99.05 (37), 145.09 (100), 157.09 (58), 175.10 (2), 319.19 (13), 495.30 (18)	Achyranthesterone A[a]	+	+
A2	9.55	541.3037	495.2986	$+HCOO^-$	2.976	$C_{27}H_{44}O_8$	HCD80: 145.09 (100), 175.10 (1), 319.19 (23), 495.30 (12)	Unknown	+	−
A3	10.61	541.3038	495.2979	$+HCOO^-$	−0.724	$C_{27}H_{44}O_8$	HCD80: 145.09 (100), 175.10 (1), 319.19 (23), 495.30 (13)	Unknown	+	−
A4	15.95	555.3188	509.3124	$+HCOO^-$	2.426	$C_{28}H_{46}O_8$	HCD80: 159.10 (100), 189.11 (1), 319.19 (13), 509.31 (12)	Unknown	+	−
A5	19.03	537.308	491.3033	$+HCOO^-$	2.191	$C_{28}H_{44}O_8$	HCD80: 141.09 (66), 319.19 (100), 391.21 (46), 491.30 (60)	Unknown	+	−
B1	8.4	541.3038	495.2979	$+HCOO^-$	3.076	$C_{27}H_{44}O_8$	HCD100: 83.05 (51), 175.10 (100), 319.19 (20), 495.30 (10)	Podecdysone C[a]	−	+
B2	8.62	557.2982	511.2917	$+HCOO^-$	2.561	$C_{27}H_{44}O_9$	HCD100: 83.05 (28), 175.10 (100), 335.19 (25), 511.29 (57)	Unknown	−	+
B3	8.88	541.3036	495.2981	$+HCOO^-$	2.876	$C_{27}H_{44}O_8$	HCD100: 83.05 (52), 175.10 (100), 319.19 (21), 495.30 (5)	Unknown	−	+
B4	11.48	541.3033	495.2983	$+HCOO^-$	2.576	$C_{27}H_{44}O_8$	HCD80: 83.05 (19), 159.10 (100), 317.18 (50), 335.19 (13), 495.30 (32) HCD100: 83.05 (79), 159.10 (100)	Unknown	−	+
B5	13.31	555.3188	509.3129	$+HCOO^-$	2.426	$C_{28}H_{46}O_8$	HCD100: 97.07 (58), 189.11 (100), 319.19 (16), 509.31 (3)	Unknown	−	+
B6	13.79	525.3084	479.3034	$+HCOO^-$	2.591	$C_{27}H_{44}O_7$	HCD80: 83.05 (17), 159.10 (100), 319.19 (26), 479.30 (14) HCD100: 83.05 (81), 159.10 (100), 319.19 (19)	Rhapontisterone B or isomer	−	+
B7	13.9	511.2927	465.2865	$+HCOO^-$	2.541	$C_{26}H_{42}O_7$	HCD80: 83.05 (12), 145.09 (100), 319.19 (60), 465.29 (53)	Unknown	−	+
B8	14.46	555.3129	509.3129	$+HCOO^-$	−3.474	$C_{28}H_{46}O_8$	HCD100: 97.07 (63), 189.11 (100), 319.19 (22), 509.31 (8)	Unknown	−	+
B9	14.74	539.2888	493.2813	$+HCOO^-$	3.726	$C_{27}H_{42}O_8$	HCD100: 83.05 (41), 159.10 (53), 333.17 (100), 493.28 (82)	Unknown	−	+
B10	15.5	555.3188	509.3118	$+HCOO^-$	2.426	$C_{28}H_{46}O_8$	HCD80: 189.11 (100), 319.19 (20), 509.31 (40) HCD100: 97.07 (58), 189.11 (100)	Unknown	−	+
B11	16.15	523.292	477.2869	$+HCOO^-$	1.841	$C_{27}H_{42}O_7$	HCD100: 83.05 (80), 159.10 (100), 317.18 (74), 477.29 (11)	Unknown	−	+
B12	16.29	569.3345	523.3286	$+HCOO^-$	3.076	$C_{29}H_{48}O_8$	HCD80: 203.13 (100), 319.19 (26), 523.33 (26) HCD100: 111.08 (66), 203.13 (100), 319.19 (49)	Unknown	−	+
B13	16.37	541.3035	495.2961	$+HCOO^-$	2.776	$C_{27}H_{44}O_8$	HCD80: 83.05 (5), 159.10 (31), 335.19 (1), 391.125 (100), 495.30 (4) HCD100: 83.05 (32), 159.10 (100), 231.14 (53)	Unknown	−	+
B14	17.25	525.3076	479.297	$+HCOO^-$	4.191	$C_{27}H_{44}O_7$	HCD100: 83.05 (64), 159.10 (100), 319.19 (45), 479.30 (4)	*β*-Ecdysterone[a]	−	+
B15	17.52	541.3011	495.2961	$+HCOO^-$	−0.724	$C_{27}H_{44}O_8$	HCD100: 83.05 (51), 159.10 (100), 335.19 (53), 495.30 (5)	Polypodine B[a]	−	+
B16	18.7	569.3351	523.3276	$+HCOO^-$	3.076	$C_{29}H_{48}O_8$	HCD100: 83.05 (51), 145.09 (100), 203.13 (2), 319.19 (20), 523.33 (22)	Unknown	−	+
B17	19.08	525.3088	479.3012	$+HCOO^-$	4.191	$C_{27}H_{44}O_7$	HCD80: 159.10 (100), 319.19 (64), 479.30 (63)	Rhapontisterone B or isomer	−	+

Continued

No.	t_R/min	*m/z*	M − H	Adducts	Delta mmu	Molecular formula	MS/MS fragment ions	Identification	C21-OH	C25-OH
							HCD100: 83.05 (41), 159.10 (100)			
B18	19.12	523.2932	477.2872	+HCOO$^-$	3.041	$C_{27}H_{42}O_7$	HCD100: 83.05 (67), 159.10 (100), 245.16 (97), 317.18 (41), 477.29 (23)	Unknown	−	+
B19	19.19	525.3082	479.3014	+HCOO$^-$	4.191	$C_{27}H_{44}O_7$	HCD100: 83.05 (60), 159.10 (100), 319.19 (53), 479.30 (10)	Rhapontisterone B or isomer	−	+
B20	19.31	539.324	493.3202	+HCOO$^-$	−1.459	$C_{28}H_{46}O_7$	HCD80: 173.12 (100), 319.19 (55), 493.32 (43)	Unknown	−	+
							HCD100: 97.07 (54),173.12 (100)			
B21	19.35	539.3247	493.3187	+HCOO$^-$	−1.459	$C_{28}H_{46}O_7$	HCD100: 97.07 (94), 173.12 (100), 319.19 (43), 493.32 (5)	Unknown	−	+
B22	19.41	525.309	479.3014	+HCOO$^-$	4.191	$C_{27}H_{44}O_7$	HCD100: 83.05 (73), 159.10 (100), 319.19 (44), 479.30 (5)	Rhapontisterone B or isomer	−	+
B23	19.45	539.3237	493.319	+HCOO$^-$	−1.459	$C_{28}H_{46}O_7$	HCD100: 97.07 (100), 173.12 (99), 319.19 (32), 493.32 (4)	Unknown	−	+
B24	15.44	687.361	641.3551	+HCOO$^-$	2.367	$C_{33}H_{54}O_{12}$	HCD100: 83.05 (47), 159.10 (100), 319.19 (69), 479.30 (19)	*β*-Ecdysterone-Glc or isomer	−	+
C1	11.88	511.2925	511.2925	−H	2.341	$C_{27}H_{44}O_9$	HCD80: 175.10 (64), 261.15 (87), 279.16 (100), 335.19 (28), 511.29 (88)	Unknown	−	−
C2	13.26	541.3023	495.2963	+HCOO$^-$	1.576	$C_{27}H_{44}O_8$	HCD80: 159.10 (100), 317.18 (100), 335.19 (2), 495.30 (3)	Unknown	−	−
C3	14.09	541.3032	495.2982	+HCOO$^-$	2.476	$C_{27}H_{44}O_8$	HCD80: 175.10 (60), 317.18 (98), 319 (15), 391.25 (100), 495.30 (54)	Unknown	−	−
C4	14.34	687.3605	641.355	+HCOO$^-$	1.867	$C_{33}H_{54}O_{12}$	HCD80: 101.02 (100), 159.10 (31), 319.19 (48), 479.30 (54)	25*R*-inkosterone-Glc or isomer	−	−
C5	15.17	687.361	641.3551	+HCOO$^-$	2.367	$C_{33}H_{54}O_{12}$	HCD80: 89.02 (100), 113.02 (85), 159.10 (55), 319.19 (77), 479.30 (47)	25*R*-inkosterone-Glc or isomer	−	−
C6	15.71	687.361	641.3551	+HCOO$^-$	2.367	$C_{33}H_{54}O_{12}$	HCD100: 85.03 (14), 101.02 (89), 113.02 (49), 159.10 (100), 319.19 (94), 479.30 (12)	25*R*-inkosterone-Glc or isomer	−	−
C7	16.53	687.3616	641.3551	+HCOO$^-$	2.967	$C_{33}H_{54}O_{12}$	HCD80: 89.02 (100), 101.02 (72), 113.02 (87), 159.10 (53), 319.19 (91), 479.30 (64)	25*R*-inkosterone-Glc or isomer	−	−
C8	16.73	687.3616	641.3551	+HCOO$^-$	2.967	$C_{33}H_{54}O_{12}$	HCD100: 85.03 (94), 101.02 (100), 159.10 (94), 319.19 (84), 479.30 (11)	25*R*-inkosterone-Glc or isomer	−	−
C9	16.93	525.3077	479.3011	+HCOO$^-$	1.891	$C_{27}H_{44}O_7$	HCD80: 159.10 (100), 319.19 (82), 479.30 (67)	Unknown	−	−
C10	17.92	687.3611	641.3543	+HCOO$^-$	2.467	$C_{33}H_{54}O_{12}$	HCD100: 85.03 (41), 101.02 (44), 113.02 (35), 159.10 (81), 319.19 (100), 479.30 (11)	25*R*-inkosterone-Glc or isomer	−	−
C11	18.09	525.3083	479.297	+HCOO$^-$	4.191	$C_{27}H_{44}O_7$	HCD80: 159.10 (100), 319.19 (94), 479.30 (64)	25*R*-inkosterone[a]	−	−
C12	18.55	525.3079	479.297	+HCOO$^-$	4.191	$C_{27}H_{44}O_7$	HCD80: 159.10 (100), 319.19 (86), 479.30 (62)	25*S*-inkosterone[a]	−	−
C13	19.23	495.2974	495.298	−H	4.755	$C_{27}H_{44}O_8$	HCD80: 159.10 (18), 261.15 (94), 279.17 (100), 335.19 (27), 495.30 (59)	Unknown	−	−
C14	19.64	539.3245	493.3211	+HCOO$^-$	−1.459	$C_{28}H_{46}O_7$	HCD100: 85.03 (78), 173.12 (100), 319.19 (99), 493.32 (13)	Unknown	−	−
C15	19.74	523.2928	477.2865	+HCOO$^-$	−0.159	$C_{27}H_{42}O_7$	HCD80: 159.10 (33), 317.18 (37), 477.29 (100)	Unknown	−	−
C16	19.82	525.3086	479.3014	+HCOO$^-$	4.191	$C_{27}H_{44}O_7$	HCD80: 159.10 (100), 319.19 (86), 479.30 (61)	Unknown	−	−
C17	20.81	523.293	477.2865	+HCOO$^-$	−0.159	$C_{27}H_{42}O_7$	HCD80: 157.09 (17), 319.19 (60), 477.29 (100)	Unknown	−	−
C18	20.82	553.302	507.2952	+HCOO$^-$	1.276	$C_{28}H_{44}O_8$	HCD80: 85.03 (19), 159.10 (100), 301.18 (53), 319.19 (93)	Unknown	−	−

[a] identified by phytochemical isolation

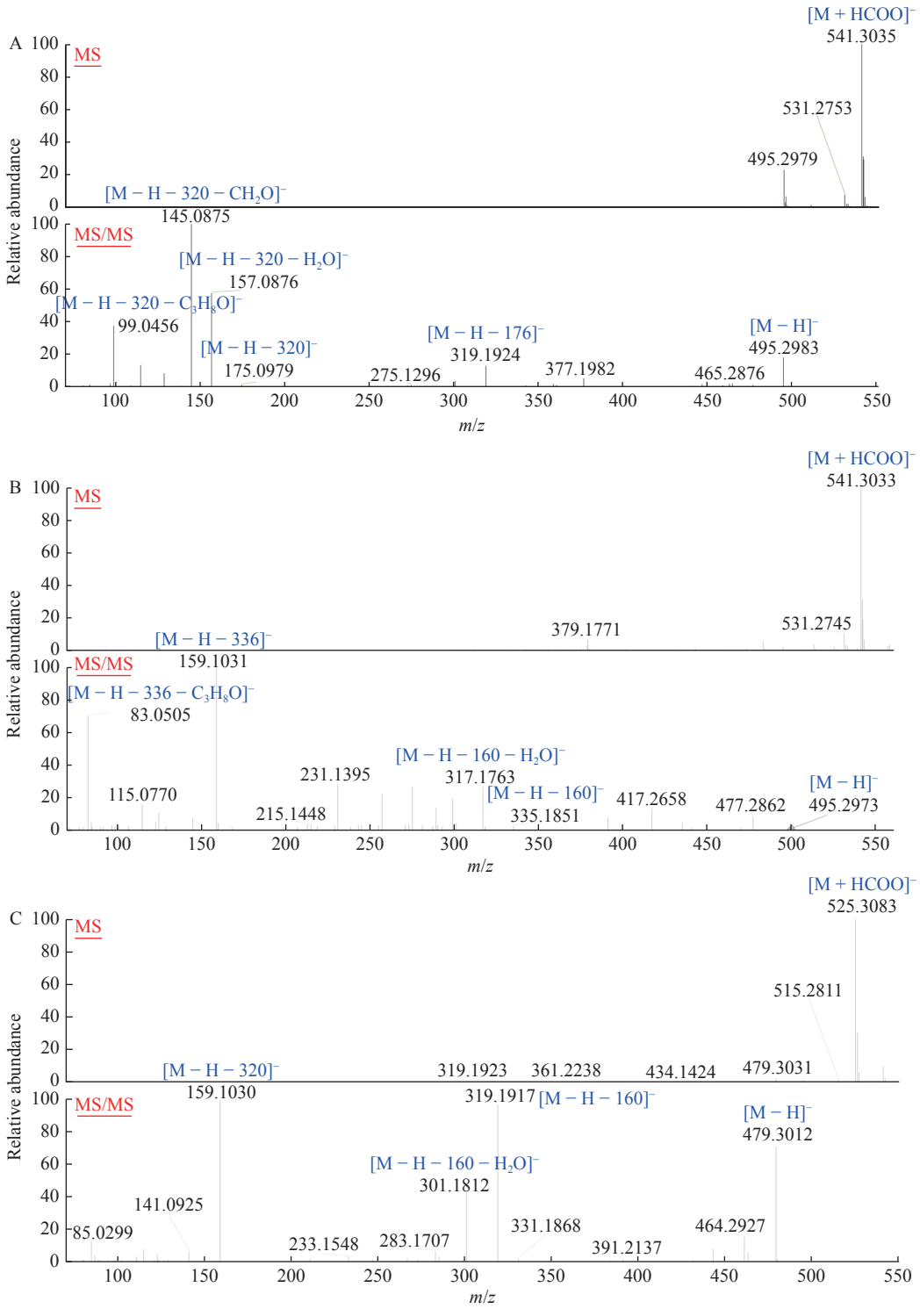

Fig. 4 The negative-mode HR-ESI-MS spectrum of A1 (A), B4 (B), and C5 (C)

The characteristic NLs of 30.01 (CH_2O) were observed between product ions *m/z* 175.10 and 145.09. Therefore, **A1** was attributed to class A. DPIs at *m/z* 319.19 and 175.10 $[M - H - 320\ Da]^-$ were the complementary ion pair, indicating the skeleton and side chain respectively. Ions at *m/z* 157.09, and 99.05 were obviously acquired by the NLs of H_2O, and $C_3H_8O_2$ from *m/z* 175.10. Furthermore, according to the in-house database of phytoecdysteroids which were isolated from *A. bidentata* in previous reports (Supporting information Table S1) and their retention time, **A1** was tentatively characterized as achyranthesterone A.

Characterization of compounds in class B

Totally, 24 phytoecdysteroids (**B1**−**B24**) were considered as class B. **B4** was given as an example, which pro-

duced $[M + HCOO]^-$ at *m/z* 541.3033 with a molecular formula of $C_{27}H_{44}O_8$. As shown in Fig. 4B, the fragment ions of *m/z* 335.19 and 317.18 were the DPIs of the skeleton, while *m/z* 159.10 and 83.05 were the DPIs of the side chain with hydroxy group at C-25. In addition, *m/z* 317.18 was generated by the NL of H_2O from *m/z* 335.19, and *m/z* 83.05 was produced by the NL of $C_3H_8O_2$ on the side chain. So **B4** was recognized as class B. Accordingly, after searching the database of phytoecdysteroids in *A. bidentata*, only polypodine B exhibited those structural characteristics. However, its retention time was inappropriate. This means that **B4** was a potential new compound. Hence, **B4** was not fully characterized.

Characterization of compounds in class C

As shown in Table 1, compounds **C1**−**C18** were categorized into class C. Taking **C5** for an example, the MS spectra of **C5** showed $[M + HCOO]^-$ at *m/z* 525.3083 with a molecular formula of $C_{27}H_{44}O_7$. In its MS/MS spectra, the fragment ions at *m/z* 159.10, 301.18, 319.19 and 479.30 showed strong intensity (Fig. 4C). Obviously, *m/z* 159.10, 301.18 and 319.19 were the DPIs of phytoecdysteroids, and *m/z* 479.30 was the $[M - H]^-$ of **C5**. Futhermore, there were neither typical NLs of CH_2O, $C_3H_8O_2$ and $C_3H_8O_3$, nor DPIs of *m/z* 83.05 and 97.07. As a result, **C5** was categorized as class C. Then, 25*R*-inkosterone and 25*S*-inkosterone were filtered by the *m/z* and chemical structure with the database of phytoecdysteroids in *A. bidentata.* Finally, **C5** was unambiguously identified as 25*R*-inkosterone by comparing with the reference standard.

Targeted isolation and structural elucidation of new compounds A2, A3 and C18

Compounds **A2** and **A3** with the same molecular formula of $C_{27}H_{44}O_8$ were characterized as the isomers of achyranthesterone A due to the NLs of 30.01 (CH_2O) and DPIs at *m/z* 319.19 and 175.10 (Supporting information Figs. S2A−S2B). According to the DPIs at *m/z* 319.19 and 159.10 without other representative NLs or DPIs (Supporting information Fig. S2C), compound **C18** with the molecular formula of $C_{28}H_{44}O_8$ was categorized to class C. Through searching the in-house database (Supporting information Table S1), they were potentially novel. In order to validate the structures of **A2**, **A3** and **C18**, the compounds were purified from *A. Bidentata* through targeted isolation.

The planar structures of **A2** and **A3** were established according to the key ^{1}H-^{1}H COSY and HMBC correlations as indicated in Fig. 5A. The ^{1}H-^{1}H COSY spectrum showed correlations between H-22/H-23, H-23/H-24, H-24/H-25, H-25/H-26 and H-25/H-27, together with the HMBC cross-peaks in H-27/C-24, H-27/C-25 and H-27/C-26, indicating the substitution of the eight-carbon polyol side chain. Moreover, the HMBC cross-peaks of H-17/C-20, H-17/C-21, H-17/C-22, H-21/C-17, H-21/C-20 and H-21/C-22, suggested the side chain linked on C-17.

The NOESY data and ^{1}H-^{1}H coupling constants were used to determine the stereochemistry of **A2** as indicated in Fig. 5B. The H-19/ H_β-11, H-19/H_β-1, and H-19/H_β-5 correlations in the NOESY spectrum established the *cis*-type junctions of rings A and B. The H_β-11/H-18, H_β-15/H-18, H_β-12/H-18, and H-9/H_α-12 cross-peaks confirmed the *trans*-type junctions of rings C and D. Compared with 25*R*-inkosterone and 25*S*-inkosterone, the chemical shifts of C-25, 26, and 27 of **A2** were closely similar with those of 25*R*-inkosterone (Table 2 and Supporting Information Table S2). Thus, C-25 in **A2** was confirmed as *R*-configuration and identified as (20*S*,22*R*,25*R*)-2β,3β,14α,20β,21,22β,26-heptahydroxy-5β-ergost-7-en-6-one, named achyranthesterone B. The NMR data indicated that the resonances of C-24/C-27 displayed relatively larger variation between **A3** (δ_C 32.3/17.5) and **A2** (δ_C 31.6/16.9) (Table 2). These results demonstrated that the ste-

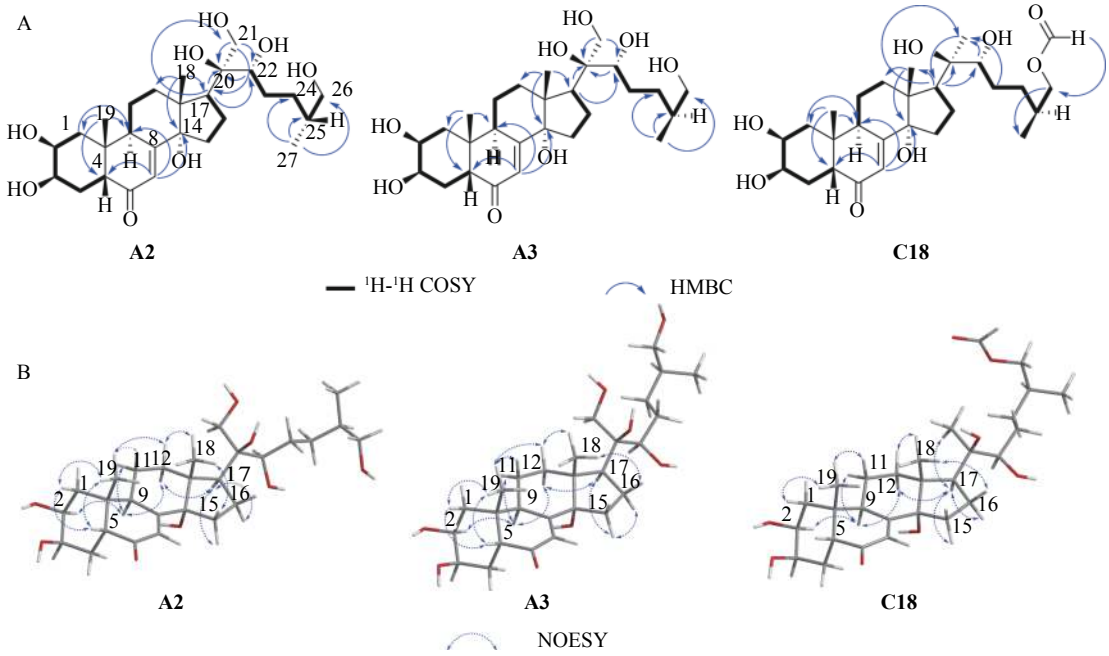

Fig. 5 Key ^{1}H-^{1}H COSY (A), HMBC (A), and NOESY (B) correlations of A2, A3 and C18

Table 2 ^{1}H and ^{13}C NMR data of A2, A3 and C18 (δ in ppm, *J* in Hz)

Position	A2 (CD_3OD)		A3 (CD_3OD)		C18 (C_5D_5N)	
	δ_C	δ_H	δ_C	δ_H	δ_C	δ_H
1*α*	37.4	1.81 m	37.4	1.81 m	38.4	2.07 m
1*β*		1.47 m		1.46 m		1.94 m
2	68.7	3.82 m	68.7	3.81 m	68.5	4.20 m
3	68.5	3.98 m	68.5	3.98 m	68.4	4.25 m
4	32.9	1.81 m	32.9	1.81 m	32.8	1.80 m
5	51.8	2.41 m	51.8	2.42 m	51.8	3.04 (dd, 3.8, 13.2)
6	206.5		206.4		203.0	
7	122.2	5.84 (d, 2.5)	122.2	5.84 (d, 2.5)	122.1	6.28 (d, 2.1)
8	167.9		167.8		166.4	
9	35.1	3.16 m	35.1	3.17m	34.8	3.62 m
10	39.3		39.3		39.1	
11*α*	21.5	1.81 m	21.5	1.81 m	21.5	1.94 m
11*β*		1.74 m		1.73 m		1.80 m
12*α*	31.8	2.11 m	31.8	2.10 m	32.2	2.63 (dt, 4.8, 13.0)
12*β*		1.47 m		1.81 m		2.07 m
13	48.3		48.3		48.5	
14	85.3		85.3		84.6	
15*α*	31.6	1.99 m	31.6	2.00 m	32.4	2.17 m
15*β*		1.63 m		1.73 m		2.07 m
16*α*	21.6	1.81 m	21.6	2.10 m	22.0	2.48 m
16*β*		1.74 m		1.73 m		1.94 m
17	48.2	2.41 m	48.2	2.42 m	50.4	2.94 (t, 9.2)
18	18.0	0.92 s	18.0	0.92 s	18.3	1.25 s
19	24.4	0.99 s	24.4	0.99 s	24.8	1.10 s
20	78.6		78.6		77.1	
21	67.1	3.82 m	67.1	3.81 m	21.8	1.59 s
22	78.7	3.47 brs	79.1	3.47 (d, 11.0)	77.3	3.82 (d, 10.5)
23*α*	30.4	1.74 m	30.5	1.81 m	30.2	1.80 m
23*β*		1.47 m		1.46 m		1.53 m
24*α*	32.0	1.63 m	32.3	1.81 m	32.1	1.94 m
24*β*		1.47 m		1.16 m		1.36 m
25	36.8	1.63 m	37.0	1.64 m	33.2	1.80 m
26*α*	68.6	3.47 m	68.2	3.51 (dd, 11.0, 6.0)	68.9	4.13 (dd, 4.5, 10.8)
26*β*		3.39 m		3.39 m		3.99 (dd, 6.6, 10.8)
27	16.9	0.97 (d, 6.5)	17.5	0.98 (d, 7.5)	17.7	0.86 (d, 6.7)
28					162.1	8.29 s

Measured at 500 (^{1}H) and 125 (^{13}C) MHz

reocenter of C-25 of **A3** was opposite to **A2**. Thus, compound **A3** was identified as the C-25 epimer of **A2** and elucidated as (20*S*,22*R*,25*S*)-2*β*,3*β*,14*α*,20*β*,21,22*β*,26-heptahydroxy-5*β*-ergost-7-en-6-one, named achyranthesterone C.

The ^{13}C NMR signals of C-1 to C-19 for **C18** (Table 2) revealed that they almost shared identical chemical shifts as those of compound 25*S*-inkosterone. Compared with **7** [H-26 (δ_H 3.45, 3.33) and C-26 (δ_C 68.1)], the H-26 (δ_H 4.13, 3.99) of **C18** down-field shifted by 0.68 and 0.66 ppm, and C-26 (68.9) down-field shifted by 0.8 ppm, respectively. The above-mentioned signals suggested that 26-OH was methyl esterified, which was verified by the HMBC correlations from H-26 to C-28.

In an attempt to determine the stereochemistry of C-25, compound **C18** was hydrolyzed and compared with 25*R*-inkosterone and 25*S*-inkosterone. The result showed that the retention time of hydrolysis product of **C18** was identical to 25*S*-inkosterone (Supporting Information Figs. S3−S4). Thus,

the C-25 of **C18** was determined to be *S*-configuration and characterized as (20*S*,22*R*,25*S*)-2*β*,3*β*,14*α*,20*β*,21,22*β*-pentahydroxy-26-formate-5*β*-ergost-7-en-6-one, named achyranthesterone D.

Conclusion

In the current study, UHPLC-LTQ-Orbitrap was used to establish a rapid and simple strategy for characterization of phytoecdysteroids. On account of the diverse diagnostic product ions (DPIs) [eg. *m/z* 335.19, 319.19, 175.10, 145.10, 83.05, 97.07] or neutral losses (NLs) of 30 Da (CH_2O) [eg. *m/z* 175.10→145.09], 76 Da ($C_3H_8O_2$) [eg. *m/z* 159.10→83.05] and 92 Da ($C_3H_8O_3$) [eg. *m/z* 175.10→83.05], phytoecdysteroids are categorized into three classes. A total of 47 compounds, most of which are potential new compounds, are unambiguously or tentatively characterized from *Achyranthes bidentata* Blume, including 5 compounds in class A, 24 compounds in class B, and 18 compounds in class C. Three new phytoecdysteroids are isolated and identified to validate the reliability of this strategy. This study summarizes the fragmentation behaviors of phytoecdysteroids and provides reference for the discovery of new compounds.

Supporting Information

Supporting information of this paper can be requested by sending E-mails to the corresponding authors.

References

[1] Jaiswal Y, Liang ZT, Ho A, *et al*. Tissue-based metabolite profiling and qualitative comparison of two species of Achyranthes roots by use of UHPLC-QTOF-MS and laser microdissection [J]. *J Pharm Anal*, 2018, **8**(1): 10-19.

[2] Shen LJ, Luo KD, Wen XX, *et al*. Systematic chemical characterization of Xiexin decoctions using high performance liquid chromatography coupled with electrospray ionization mass spectrometry [J]. *Chin J Nat Med*, 2021, **19**(6): 464-472.

[3] Zou D, Zhang AH, Yan GL, *et al*. UPLC-MS coupled with a dynamic multiple data processing method for the comprehensive detection of the chemical constituents of the herbal formula San-miao-wan [J]. *Anal Methods*, 2014, **6**(9): 2848.

[4] Sumner LW, Amberg A, Barrett D, *et al*. Proposed minimum reporting standards for chemical analysis Chemical Analysis Working Group (CAWG) Metabolomics Standards Initiative (MSI) [J]. *Metabolomics*, 2007, **3**(3): 211-221.

[5] Suh KS, Lee YS, Choi EM. The protective effects of *Achyranthes bidentata* root extract on the antimycin A induced damage of osteoblastic MC3T3-E1 cells [J]. *Cytotechnology*, 2014, **66**(6): 925-935.

[6] Jiang YN, Zhang YQ, Chen WH, *et al*. *Achyranthes bidentata* extract exerts osteoprotective effects on steroid-induced osteonecrosis of the femoral head in rats by regulating RANKL/RANK/OPG signaling [J]. *J Transl Med*, 2014, **12**: 334.

[7] Hua S, Zhang X. Effects of *Achyranthes bidentata* alcohol on proliferation capacity of osteoblasts and miRNA in Runx2 [J]. *Exp Ther Med*, 2019, **18**(3): 1545-1550.

[8] Chen Z, Wu G, Zheng R. A systematic pharmacology and *in vitro* study to identify the role of the active compounds of *Achyranthes bidentata* in the treatment of osteoarthritis [J]. *Med Sci Monitor*, 2020, **26**: e925545.

[9] Siu WS, Shum WT, Cheng W, *et al*. Topical application of Chinese herbal medicine DAEP relieves the osteoarthritic knee pain in rats [J]. *Chin Med*, 2019, **14**: 55.

[10] Jung SK, Choi DW, Kwon DA, *et al*. Oral administration of Achyranthis Radix extract prevents tma-induced allergic contact dermatitis by regulating th2 cytokine and chemokine production *in vivo* [J]. *Molecules*, 2015, **20**(12): 21584-21596.

[11] Wang Y, Xu Y, Pan Y, *et al*. Radix *Achyranthis bidentatae* improves learning and memory capabilities in ovariectomized rats [J]. *Neural Regen Res*, 2013, **8**(18): 1644-1654.

[12] Liu CM, Chen HJ, Chen K, *et al*. Sulfated modification can enhance antiviral activities of *Achyranthes bidentata* polysaccharide against porcine reproductive and respiratory syndrome virus (PRRSV) *in vitro* [J]. *Int J Biol Macromol*, 2013, **52**: 21-24.

[13] Jin LQ, Zheng ZJ, Peng Y, *et al*. Opposite effects on tumor growth depending on dose of *Achyranthes bidentata* polysaccharides in C57BL/6 mice [J]. *Int Immunopharmacol*, 2007, **7**(5): 568-577.

[14] Wang CS, Hua DH, Yan CY. Structural characterization and antioxidant activities of a novel fructan from *Achyranthes bidentata* Blume, a famous medicinal plant in China [J]. *Ind Crop Prod*, 2015, **70**: 427-434.

[15] Li MY, Zhu Y, Peng WQ, *et al*. *Achyranthes bidentata* polypeptide protects schwann cells from apoptosis in hydrogen peroxide-induced oxidative stress [J]. *Front Neurosci*, 2018, **12**: 868.

[16] Yang L, Jiang H, Yan ML, *et al*. A new phytoecdysteroid from the roots of *Achyranthes bidentata* Bl [J]. *Nat Prod Res*, 2017, **31**(9): 1073-1079.

[17] Zhang M, Zhou ZY, Wang J, *et al*. Phytoecdysteroids from the roots of *Achyranthes bidentata* Blume [J]. *Molecules*, 2012, **17**(3): 3324-3332.

[18] Wang QH, Yang L, Jiang H, *et al*. Isolation and identification of steroid components in *Achyranthes bidentata* Blume [J]. *Acta Chin Med Pharmacol*, 2012, **40**(1): 69-71.

[19] Wang QH, Yang L, Jiang H, *et al*. Three new phytoecdysteroids containing a furan ring from the roots of Achyranthes bidentata Bl [J]. *Molecules*, 2011, **16**(7): 5989-5997.

Cite this article as: WANG Ying-Ying, LI Jia-Yuan, YAO Chang-Liang, ZHANG Jian-Qing, YU Yang, YAO Shuai, GAO Min, WU Shi-Fei, WEI Wen-Long, BI Qi-Rui, GUO De-An. Deep chemical identification of phytoecdysteroids in *Achyranthes bidentata* Blume by UHPLC coupled with linear ion trap-Orbitrap mass spectrometry and targeted isolation [J]. *Chin J Nat Med*, 2022, **20**(7): 551-560.

Prof. GUO De-An was graduated with his Ph.D. degree of pharmacognosy from Beijing Medical University in 1990. He currently serves as director of National Engineering Research Center for TCM Standardization Technology in Shanghai Institute of Materia Medica. His research mainly focuses on the quality control and elaboration of pharmacopoeia standards for Chinese herbal medicines. To date, he has published over 700 academic papers, among which 500 plus are cited in SCI journals with 13 000 citations.